TELKOMNIKA Indonesian Journal of Electrical Engineering
Vol. 12, No. 8, August 2014, pp. 6190 ~ 6197
DOI: 10.11591/telkomnika.v12i8.4706

Slice Interpolation for MRI Using Disassemble-Reassemble Method

Qinghua Lin*[1], Min Du[1,2], Yuemin Gao[2]
[1]College of Electrical Engineering and Automation, Fuzhou University
[2]Fujian Key Lab of Medical Instrument and Pharmaceutical Technology, Fuzhou University,
2 Xue Yuan Road, University Town, Fuzhou, Fujian 350108, P. R. CHINA, +86 591 93759450
*Corresponding author, e-mail: fzulins211@163.com

Abstract

Due to physical limitations inherent in Magnetic resonance image (MRI) scanners, the inter-slice resolution of MRI is coarse. Thus, interpolation is often used to compensate it. MRI corresponds to a thin slice through the human body, and contains all the information in the slice. Based on this characteristic, a novel slice interpolation algorithm using disassemble-reassemble (D-R) method is proposed for doing MRI slice interpolation. The algorithm first disassembles all the information contained in MRI, and then reassembles them under a heuristic approach of neighborhood consistency to get higher inter-slice resolution. Series virtual images that imitate the characteristic of MRI were used to explain the principle of proposed algorithm, and the process of proposed algorithm was derived from detail analysis. Finally, we performed a large number of interpolation experiment and compared the proposed algorithm to several other interpolation techniques. Results show that the proposed algorithm outperforms the other interpolation algorithms, which means the D-R method is more suitable for MRI interpolation.

Keywords*: disassemble-reassemble method, MRI, slice interpolation*

1. Introduction

Magnetic Resonance Image (MRI) is a tomography imaging modality for producing images of a slice through the human body and can be used to visualize internal structures of the body in detail. MRI has the follow advantages: provides good contrast between the different soft tissues; can image in any plane and doesn't use ionizing radiation. These advantages let MRI be used widely in clinical purposes and medical science. But due to the MRI technical characteristic, image time acquisition and patient dose considerations, traditionally MRI are acquired as high resolution 2D slices with relatively large slice thickness in comparison to the inter-slice resolution. As shown in Figure 1, these images are three neighboring MRI of human head got from hospital. In the DICOM information of these images, the 'Manufacturer' is 'GE MEDICAL SYSTEMS', the 'Institution Name' is 'Fujian Tumor Hospital', the 'Rows and Columns' are both '512', the 'Slice Thickness' is '5mm', and the 'Space Between Slices' is '6mm'. For these images, the inter-slice resolution is '6mm', and intra-slice one is less than '1mm'. The inter-slice resolution of these images were coarse, thus many image-processing applications (such as image visualization and accurate quantitative analysis) need some kinds of interpolation between the slices.

There are many slice interpolation algorithms proposed in literatures. Broadly, these interpolation algorithms can be divided into two categories: scene-based and object-based. The scene-based methods use the intensity values of the given scene to determine the interpolated scene intensity values. The object-based methods use the object information extracted from the given scene to guide the interpolation process. In these literatures, Thomas compared the traditional interpolation methods: 1) Truncated and windowed sinc; 2) Nearest neighbor; 3) Linear; 4) Quadratic; 5) Cubic and approximation techniques and had the conclusion that 'one might have trouble in finding the optimal kernel for a specific interpolation application' [1]. Pervez utilized amalgamation of bi-cubic interpolation and 2d interpolation filter to produce super resolution [2]. Fei used multisurface fitting to achieve image SR reconstruction framework [3]. Konstantinos imposed Hermite kernels irrespectively of the maximum order of signal

Received October 11, 2013; Revised May 18, 2014; Accepted June 3, 2014

derivative and achieved faster execution and smaller interpolation error [4, 5]. Sunil proposed a low complex content adaptive interpolation for real time application [6].

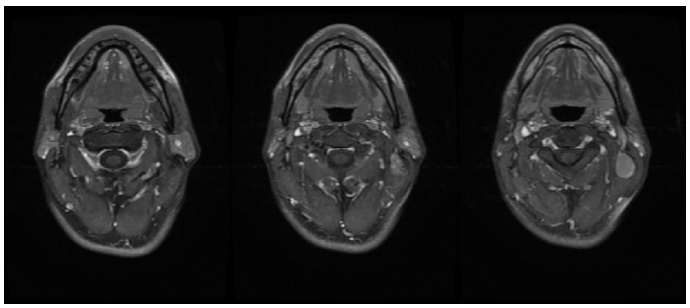

Figure 1. Three Neighboring MRI of Human Head

The algorithms proposed in literatures are algebraically demanding interpolation methods that utilized information of the values of the signal to be interpolated at distinct positions. The fundamental of these algorithms is the information of the values of the signal to be interpolated should be precise at distinct points. These algorithms are fit for photos, which is point imaging. But for MRI, this assumption is hard to achieve. MRI corresponds to a thin slice through the human body, and contains all the information in the slice. Thus means the intensive value of the given scene of MRI is for voxel, other than point. For that, the results of these methods are coarseness. The interpolation results had forges, and the edges were dimmed.

To improve the interpolation of MRI, this paper proposes a novel approach to do the MRI interpolation, which we call it as D-R method. MRI corresponds to a thin slice through the human body, and contains all the information in the slice. Based on this characteristic, the D-R method first disassembles the information contained in MRI, and then reassembles them under the heuristic approach of approaching consistency to get higher slice-resolution. Theory analysis and experiment results all proved the feasibility and effective of the proposed slice interpolation algorithm.

2. Research Method

As shown in Figure 1, the inter-slice resolution of MRI is worse. In the DICOM information of these MRI, the 'Slice Thickness' is '5mm', and the 'Space Between Slices' is '6mm'. We want to improve the inter-slice resolution of these MRI, and the 'Slice Thickness' will be '1mm'. Essentially, one '5mm' thick slice is composed by five '1mm' thin ones, likes building blocks. This gives us some tips to do the slice interpolation. Consider series images as shown in Figure 2(a). These 120 images are constructed artificial. Three concentric rings with difference diameters and grayscales are in the center of these images. Figure 2(b) is the center coronal plane of Figure 2(a). Every six images in Figure 2(a) were considered as a group. The first five images in one group compose corresponding one image in Figure 2(c), with the sixth image in the group missing. So Figure 2(c) has 20 images. Figure 2(d) is the center coronal plane of Figure 2(c). In Figure 2(c), the inter-slice resolution of the images is worse. The images have forges, and the edges are dimmed. Image-processing applications (such as image visualization and accurate quantitative analysis) need some kinds of interpolation between the slices. From the assumption, the images in Figure 2(c) contain the information of Figure 2(a). Thus, we can disassemble the images in Figure 2(c), and reassemble them as the images in Figure 2(a), and it will improve the inter-slice resolution of the images.

Base on the analysis above, we define the n images in Figure 2(c) as input images, the p*n images in Figure 2(a) as output images. The gray value at point (i,j) in the k level of input image is $f_k(i,j)$, $1 \le k \le n$, k is integer. The gray value at point (i,j) in the m level of output image is $g_m(i,j)$. $1 \le m \le p*n$, m is integer. One image in input images is composed by p images in output images. Since MRI corresponds a slice through the human body, the same human tissue has identical type of g(i,j), and identical type of $g(i,j)$ were nearby. Different human tissues have

different types of $g(i,j)$ in MRI. Without loss of generality, we assume that the pixel in input image $f(i,j)$ is combined by two types of pixels in output image $g(i,j)$ at most. If $f(i,j)$ is composed by more types of $g(i,j)$, the analysis processing is the same, but complex. Thus, we just consider the situation of two at most in this paper.

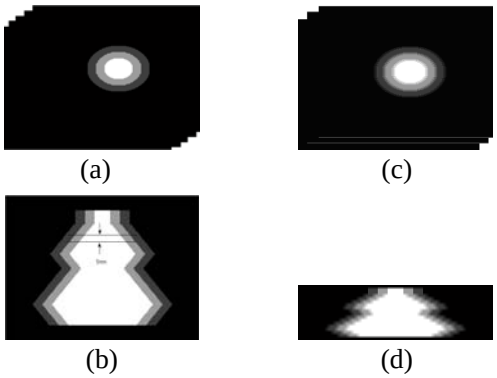

Figure 2. Imitation the Processing of MRI; (a) 120 original virtual images, (b) center coronal plane of original images, (c) 20 compose images. (d) center coronal plane of compose images

2.1. Disassemble the Input Image

The pixels in input image can be categorized into two types: smooth type and edge type. As shown in formula (1), the smooth type pixels are those pixels whose gradient are not large than the threshold, and that mean these pixels are in object. The edge type pixels are those pixels whose gradient are large than the threshold, and that mean these pixels were on the edges of objects.

$$f(i,j)=\begin{cases} S(i,j) & G(i,j)\le T \\ E(i,j) & G(i,j)>T \end{cases} \tag{1}$$

Where $S(i,j)$ is the smooth type pixels, $E(i,j)$ is the edge type pixels, $G(i,j)$ is the gradient of $f(i,j)$, T is the threshold.

For the smooth type pixels $S(i,j)$ in the input image, the corresponding $g(i,j)$ in the output image is the same, and can be derived by formula (2).

$$g(i,j)=S(i,j)/(p-1) \tag{2}$$

After all the smooth type pixels are confirmed. We come to the edge type pixels. For the edge type pixels $E(i,j)$ in the input image, it should confirm the edge belong to which two objects first. Assume $E(i,j)$ belong to two object of g' and g'', then the corresponding $g(i,j)$ in the output image can be derived by formula (3).

$$\begin{cases} E(i,j)=a*g'(i,j)+b*g''(i,j) \\ a+b=p \end{cases} \tag{3}$$

Where a and b are no negative integer. $g'(i,j)$ and $g''(i,j)$ are the gray values of g' and g''.The formula (2) is the simple situation of formula (3) where a or b is zero.

2.2. Reassemble the Input Image

For the smooth type pixels, the $g_k(i,j)$, $g_{k+1}(i,j)$, …, $g_{k+p}(i,j)$ are identical, and there are no problem of reassemble. But for the edge type pixels, the $g_k(i,j)$, $g_{k+1}(i,j)$, …, $g_{k+p}(i,j)$ are differences, and there need a heuristic approach to reassemble them. Since MRI corresponds a

slice through the human body, the same human tissue has identical type of $g(i,j)$, and identical type of $g(i,j)$ were nearby. Different human tissues have different types of $g(i,j)$ in MRI. As formula (4) or formula (5), we assume $g_k(i,j)$, $g_{k+1}(i,j)$, …, $g_{k+p}(i,j)$ are several $g'(i,j)$ and $g''(i,j)$.

$$[g_k(i,j), g_{k+1}(i,j), \cdots, g_{k+p}(i,j)] \Rightarrow [g'(i,j), \cdots g'(i,j), \ldots, g''(i,j),] \quad (4)$$

Or:

$$[g_k(i,j), g_{k+1}(i,j), \cdots, g_{k+p}(i,j)] \Rightarrow [g'(i,j), \cdots g''(i,j), \ldots, g'(i,j),] \quad (5)$$

The pixel $E(i,j)$ is edge type pixel, and belong to two objects. According to the $g(i,j)$ in one object is identical, we can decide $g'(i,j)$ is at left, or $g''(i,j)$ is at left, or it is sandwich structure.

For the missing (p**k*-1) layers, the proposed algorithm can treat it as the methods proposed in literature. In this paper, we just use the linear interpolation for simple.

2.3. Proposed Algorithm

From the theory analysis, the proposed algorithm works as follows:

1) It calculates the gradient of each pixel in input images.

2) If the gradient is large than a predefined threshold, the pixel is known as an edge type pixel, else the pixel is known as a smooth type pixel.

3) For each smooth type pixel, the gray value and position is used to decide which object the pixel belongs.

4) For each edge type pixel, the gray value and position is used to decide which two objects the pixel belongs.

5) Use formula (2) and formula (3) to disassemble the pixels.

6) Use formula (4) or (5) to reassemble the edge type pixels.

7) Use linear interpolation to reconstruct the miss layers.

8) Output the inter-slice images.

3. Results and Analysis

In order to evaluate the performance of the proposed inter-slice interpolation algorithm, we have conducted extensive experiments in comparison three other inter-slice interpolation methods: Linear interpolation, Spline interpolation and Cubic interpolation. The test environment is MATLAB 7.1. The Linear, Spline and Cubic interpolation is embedded in MATLAB 7.1, and can easy to use them. To objectively evaluate the interpolations effect, the mean absolute error (MAE) is used to give performance. The criterion is defined as follow:

$$MAE = \frac{1}{M * N} \sum \left| g(i,j) - f'(i,j) \right| \quad (6)$$

M* N was the total pixel number of the grayscale images; $g(i,j)$ is the output image; $f'(i,j)$ is the original desired image.

The first test 20 images are shown in Figure 2(c), and the images were 200*200*8 bits grayscale images. The 20 images in Figure 2(c) will be interpolated out as 120 images, and the original output images are shown in Figure 2(a). Each image in Figure 2(c) corresponds to six images in Figure 2(a). Some part of the interpolation results is shown in Figure 3. The center coronal plane of the results is shown in Figure 4, and Table 1 shows the MAE result for the above-mentioned algorithms.

In Table 1, the MAE calculated by proposed algorithm was lower than the MAE of any of the state of the art interpolation methods. For the proposed algorithm, the 28th, 38th, 58th, 68th, 88th, 98th level images were achieved by D-R method. The MAE of these images was zeros, which means the interpolation results restored the original images very well. The 18th, 48th, 78th, 108th level images were the multiple of six; from the assumption in part two, the information of these images was not contained in images of Figure 2(c), and the D-R method couldn't work. For these levels, the proposed algorithm used linear method for simple. Since the neighboring levels were restored well, the interpolation results were also acceptable. The MAE of other interpolation was bigger, which means that there were bigger difference in output images and original images. The reason for that was these algorithms utilized the intensity values of the given scene to interpolate at distinct positions. But the intensity values of the given scene were for voxels, not points. To some extent, these intensity values of the given scene were not correct at the distinct point, so the interpolation results were worse. But for the proposed algorithm, the method first disassembled the information in the given scene, and then reassembled them to get interpolated images. So the proposed algorithm works better than other art interpolation algorithms.

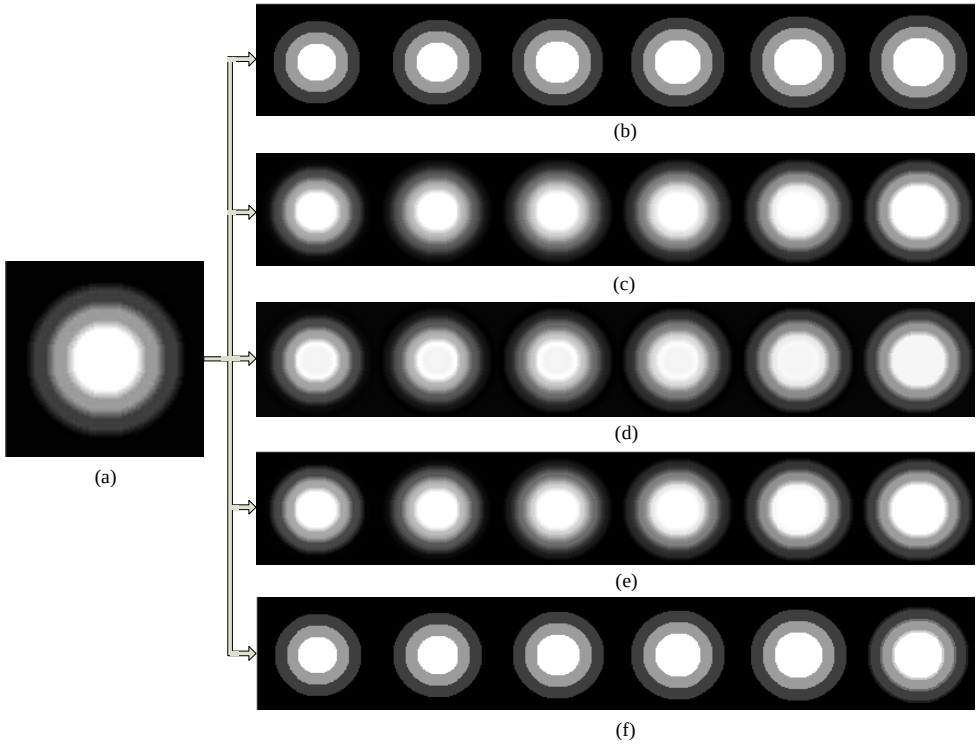

Figure 3. Some Part of the Experiment Results; (a) test image, (b) original images, (c) Linear method, (d) Spline method, (e) Cubic method, (f) proposed method.

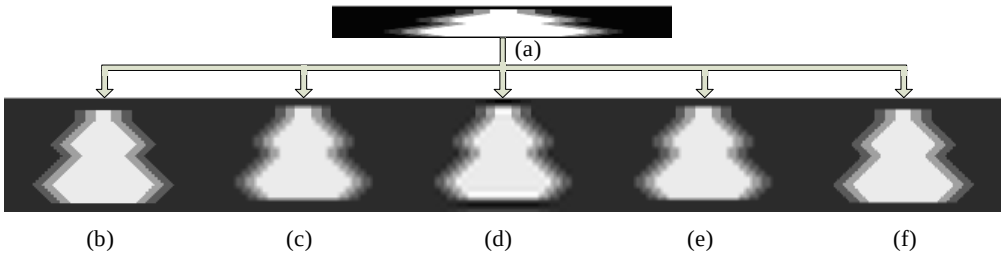

Figure 4. The Center Coronal Plane of the Experiment Results; (a) test image, (b) original images, (c) Linear method, (d) Spline method, (e) Cubic method, (f) proposed method

Table 1. MAE Comparison of Interpolated Images by Different Methods

Image	Linear	Spline	Cubic	Propose algorithm
18	4.53	4.53	4.53	0
28	9.50	9.63	9.47	0
38	17.45	17.65	17.54	0
48	19.87	19.87	19.87	0.26
58	15.13	14.62	15.13	0
68	23.46	23.67	23.15	0
78	35.42	35.42	35.42	0.31
88	42.44	44.15	42.44	0
98	31.02	33.04	31.43	0
108	5.90	5.90	5.90	2.93
…	…	…	…	…
Average	17.27	17.83	17.33	0.06

As shown in Figure 5, the second tested three MRI were the throat of human, and were extracted form Figure 1. These MRI were 33*65*8 bits grayscale images. The reason we choose human throat for experiment was that there were only two objects in images, muscle and background. So it was easy to confirm the state of pixels, muscle, background or edges. In DICOM information of these images, the 'Slice Thickness' is '5mm'. The inter-slice resolution was lower, and we wanted to improve the inter-slice resolution to '1mm'.

The interpolation results of using D-R method were shown in Figure 6. The pixels of images in the first line were disassembled and then reassembled in the next five lines images. The variations of the interpolation results were consistent with human physical.

The interpolation results of using Linear, Spline and cubic methods were shown in Figure 7. These algorithms utilized the intensity values of the given scene to be interpolated at distinct positions. So the edges in the images were coarseness and dimmed, they also have some forge areas.

Figure 5. Three Neighboring MRI of Human Throat

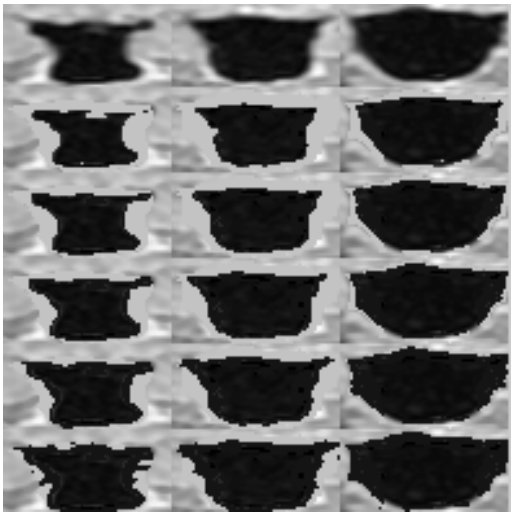

Figure 6. Interpolation Results by D-R Method

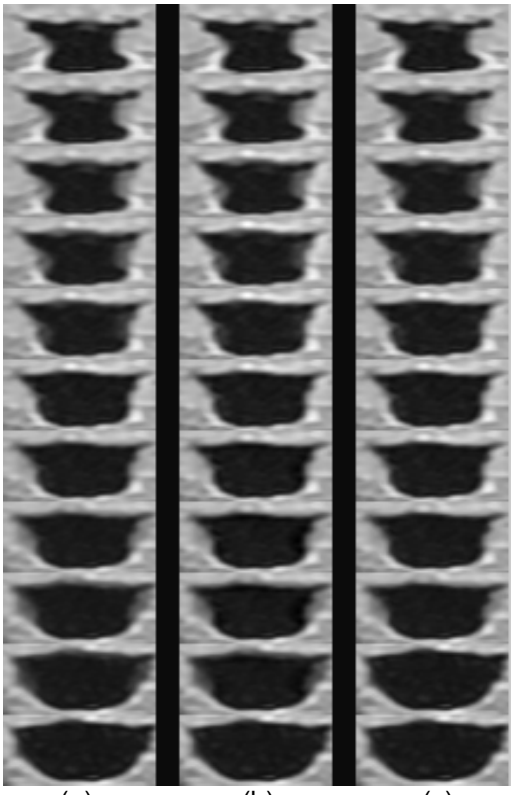

(a) (b) (c)

Figure 7. Interpolation Results by other Methods; (a) Linear method, (b) Spline method, (c) cubic method

4. Conclusion

MRI corresponds to a thin slice through the human body, and contains all the information in the slice. Thus, the intensive value of MRI is for voxels, other than points. This brings some obstacle to traditional interpolation algorithm, which needs the values of the signal to be interpolated should be precise. The interpolation results of traditional algorithms were coarseness. Based on the characteristic of MRI, this paper proposes a novel interpolation method, which is called as D-R method. The algorithm first disassembles all the information contained in MRI, and then reassembles them under the heuristic approach of approaching consistency to get higher slice-resolution. The principle and progress of the proposed algorithm are formulated in detail. The quantitative experiment results shown that the proposed algorithm outperforms the other interpolation methods, which means the D-R method is more suitable for MRI interpolation.

Acknowledgements

The authors would like to express heartfelt thanks to the financial support from the National Natural Science Foundation of China (61201397), the Program of International S&T Cooperation under Grant (S2013GR0188).

References

[1] TM Lehmann, C Gönner, et al. Survey: Interpolation Methods in Medical Image Processing. *IEEE Trans. Med. Imaging*. 1999; 18(11): 1049-1075.
[2] A Pervez, A Faisal. *A Single Image Interpolation Scheme for Enhanced Super Resolution in Bio-Medical Imaging*. Int. Conf. Bioinformatics Biomed. Eng.. Chengdu. 2010: 1-5.
[3] F Zhou, WM Yang, QM Liao. Interpolation-based image-resolution using multisurface fitting. *IEEE Trans. Image Process*. 2012; 21(7): 3312-3318.

[4] D Konstantinos K, K Aristides I, et al. *Hermite Kernels for slice interpolation in medical images*. Proc. Annu. Int. Conf. IEEE Eng. Med. Biol. Soc. San Diego. 2012: 4369-4373.
[5] KK Delibasis, AI Kechriniotis, et al. New closed formula for the univariate Hermite interpolating polynomial of total degree and its application in medical image slice interpolation. *IEEE Trans. Signal Process*. 2012; 60(12): 6294-6304.
[6] PJ Sunil, J Vinit, et al. *A low complex context adaptive image interpolation algorithm for real-time applications*. IEEE I2MTC - Int. Instrum. Meas. Technol. Conf.. Graz. 2012: 969-972.
[7] GJ Grevera, JK Udupa. Objective comparison of 3-D image interpolation methods. *IEEE Trans. Med. Imaging*. 1998; 17(4): 642-652.
[8] F Yang, Y Zhu, et al. Feature-based interpolation of diffusion tensor fields and application to human cardiac DT-MRI. *Med. Image Anal.*. 2012; 16(2): 459-481.
[9] T Philippe, B Thierry, et al. Interpolation revisited. *IEEE Trans. Med. Imaging*. 2000; 19(7): 739-758.
[10] H Gabor T, JS Zheng, et al. Shape-based interpolation. *IEEE Comput Graphics Appl.*.1992; 12(3): 69-79.
[11] Z Svitlana, R Daniel, et al. View Interpolation for Medical Images on Autostereoscopic Displays. *IEEE Trans. Circuits Syst Video Technol*. 2012; 22(1): 128-137.
[12] DH Frakes, LP Dasi, et al. A New Method for Registration-Based Medical Image Interpolation. *IEEE Trans. Med. Imaging*. 2008; 27(3): 370-377.